

A Humanized Mouse Model Generated Using Surplus Neonatal Tissue

Matthew E. Brown,^{1,2} Ying Zhou,¹ Brian E. McIntosh,³ Ian G. Norman,¹ Hannah E. Lou,¹ Mitch Biermann,⁴ Jeremy A. Sullivan,¹ Timothy J. Kamp,^{4,5} James A. Thomson,^{2,5,6} Petros V. Anagnostopoulos,⁷ and William J. Burlingham^{1,*}

¹Division of Transplantation/Department of Surgery, University of Wisconsin, Madison, WI 53792, USA

²Regenerative Biology, Morgridge Institute for Research, Madison, WI 53715, USA

³Covance Laboratories Inc., Madison, WI 53704, USA

⁴Department of Medicine, University of Wisconsin, Madison, WI 53792, USA

⁵Department of Cell & Regenerative Biology, University of Wisconsin, Madison, WI 53792, USA

⁶Department of Molecular, Cellular, & Developmental Biology, University of California, Santa Barbara, CA 93106, USA

⁷Division of Cardiothoracic Surgery/Department of Surgery, University of Wisconsin, Madison, WI 53792, USA

*Correspondence: burlingham@surgery.wisc.edu

<https://doi.org/10.1016/j.stemcr.2018.02.011>

SUMMARY

Here, we describe the NeoThy humanized mouse model created using non-fetal human tissue sources, cryopreserved neonatal thymus and umbilical cord blood hematopoietic stem cells (HSCs). Conventional humanized mouse models are made by engrafting human fetal thymus and HSCs into immunocompromised mice. These mice harbor functional human T cells that have matured in the presence of human self-peptides and human leukocyte antigen molecules. Neonatal thymus tissue is more abundant and developmentally mature and allows for creation of up to ~50-fold more mice per donor compared with fetal tissue models. The NeoThy has equivalent frequencies of engrafted human immune cells compared with fetal tissue humanized mice and exhibits T cell function in assays of *ex vivo* cell proliferation, interferon γ secretion, and *in vivo* graft infiltration. The NeoThy model may provide significant advantages for induced pluripotent stem cell immunogenicity studies, while bypassing the requirement for fetal tissue.

INTRODUCTION

Recent years have seen great progress in deriving immunodeficient mouse strains capable of being engrafted with human cells and tissues to create humanized mouse models (Lan et al., 2006; Lavender et al., 2013). These include mice modified to produce human cytokines (Rongvaux et al., 2014; Saito et al., 2016), that express specific human major histocompatibility complex (MHC) types (Shultz et al., 2010) and that do not require irradiation for xenoengraftment (McIntosh et al., 2015). While the non-T cell immune compartments within the animals are biologically relevant, humanizing these host strains via surgical implantation of human thymus tissue is required for creation of *de novo* T cells that can recognize a full complement of human MHC molecules presenting antigens *in vivo* (Shultz et al., 2012; Theocharides et al., 2016; Zhao et al., 2015). Humanized mice such as the bone marrow, liver, thymus (BLT) mouse, generated by co-transplantation of hematopoietic stem cells (HSCs) along with human fetal thymus tissue, offer a powerful translational system to study human immune responses (Hu and Yang, 2012; Kalscheuer et al., 2012; Lan et al., 2006). They are particularly useful for virology research, induced pluripotent stem cell (iPSC) immunogenicity studies, and other research requiring functional T cells selected on human self-antigen complexes (Lavender et al., 2013; Rong et al., 2014; Yu et al., 2007; Zhao

et al., 2015). Humanized models incorporating human thymus fragment implantation are uniquely suited for investigating questions relating to patient-specific immune responses to iPSC cell therapies, as self-tolerance is largely dictated by thymus-dependent mechanisms (Griesemer et al., 2010; Zhao et al., 2015).

There are multiple barriers preventing more-widespread use of the above-mentioned humanized mouse models. For example, limited fetal specimen size necessitates multiple tissue samples from divergent genetic backgrounds over an experimental course and each specimen typically yields only 15–20 humanized mice (Hassini et al., 2014). This results in significant experimental variability and discourages robust characterization of sparse and ephemeral tissue supplies. In addition, fetal tissue's immature developmental status may influence gene expression patterns, phenotype, and function of fetal tissue-derived immune cells; BLT models may not reliably represent clinical patient immune responses (Beaudin et al., 2016; Lee et al., 2011; McGovern et al., 2017; Mold and McCune, 2012; Mold et al., 2010; Notta et al., 2016).

We developed the NeoThy humanized mouse model, which utilizes abundant non-fetal human thymus tissue from neonatal cardiac surgery patients, paired with umbilical cord blood HSCs from autologous or unrelated donors. We evaluated human immune cell engraftment kinetics and their phenotype and function.





RESULTS AND DISCUSSION

Human thymus tissue was obtained from neonatal cardiac surgeries after receiving informed consent. Neonatal thymus samples provided more tissue (mean 9.3 ± 2.9 g, $n = 7$ samples, 7-day-old median age patients) compared with fetal sources (mean 0.58 g at 20 weeks gestation) (Hasini et al., 2014). This enabled cryopreservation and banking of hundreds of thymus fragments from each donor to generate humanized mice (Figure 1A). NeoThy mice were made from multiple neonatal thymus and cord blood samples and compared with fetal tissue control animals. Humanization with a 1×1 mm neonatal thymus fragment and intravenous (i.v.) injection of 0.5×10^5 – 1.5×10^5 cord blood hCD34⁺ HSCs resulted in thymic organoid formation across all four donors tested. These first-generation animals are distinguished from second-generation animals that received α hCD2 antibody (see below). The resulting thymic organoids were significantly smaller than those arising from fetal tissue (Figure 1B), yet, like fetal controls, they maintained thymic anatomy, including Hassall's corpuscles, indicating an active role in human thymopoiesis. We hypothesize that size differences between fetal and neonatal organoids may be due to variations in thymic epithelial cell progenitors within the two tissue types, rather than being the result of differential thymopoiesis efficiencies (Bleul et al., 2006).

To explore organoid function in more detail, we investigated whether the smaller organoid size affected engraftment of human immune cells in NeoThy mice. We were not able to isolate >4,000 cells from harvested NeoThy organoid explants, preventing flow cytometric analysis of the developing thymocytes. However, no significant differences in peripheral hCD45⁺, hCD19⁺, and hCD3⁺ immune cell frequency were observed between NeoThy mice and animals reconstituted with fetal thymus and cord blood HSCs (Figures 1C and 1D). Further, organoid size differences did not impact absolute numbers of CD3⁺ T cells (Figures S1A and S2B). HSC-only controls had significantly more hCD19⁺ B cells and little to no hCD3⁺ T cells at 15–18 weeks post-humanization, compared with both fetal and NeoThy mice, indicating that both models require a thymic organoid for robust T cell reconstitution. These results argue against the dysplastic murine thymus of the host animal playing a role in thymopoiesis (McDermott et al., 2010). However, we cannot conclusively rule out murine thymic tissue contributing to human T cell repopulation and function in our model.

Two strains of mice, NSG receiving 250 RAD sublethal irradiation, and NSG-W not requiring irradiation, were successfully humanized with neonatal tissues (Figure S2A), suggesting that the humanization capacity of neonatal tissues may translate well to other immunocompromised

strains. The phenotype of the engrafted human immune systems may differ depending on available cytokines, hematopoietic niches, irradiation requirements, and other specific host attributes (Brehm et al., 2010).

We used the NSG-W immunocompromised mouse for NeoThy creation because of the convenience of not having to irradiate animals. That also eliminated toxicity associated with irradiation, e.g., death and graft versus host disease (GVHD) (McIntosh and Brown, 2015). The second-generation NeoThy mice described in Figure 2 received i.v. injection of 100 μ g α hCD2 antibody on days 0 and 7 post-surgery. This method was described previously by Kalscheuer et al. (2012) for removing GVHD-associated passenger thymocytes from fetal thymic fragments. α hCD2 antibody injections delayed T cell development by approximately 4 weeks compared with first-generation NeoThy mice (Figure S3A). This delay in T cell emergence indicates that early arising T cells in BLT and other first-generation humanized mice may be partially derived from passenger thymocytes rather than *de novo* from injected HSCs educated on thymic fragment epithelial cells. As passenger thymocytes within the fragment may have already reached their final stages of development without encountering mouse xenoantigens, first-generation mice may be more prone to GVHD than second-generation mice in which *de novo* human T cells mature in the presence of mouse xenoantigens (Kalscheuer et al., 2012; Lockridge et al., 2013).

To assess whether second-generation NeoThy mice were susceptible to GVHD, we followed a cohort of five NeoThy mice for 32 weeks post-humanization (Figure 2A). At 32 weeks, five of five mice survived while maintaining human immune cell reconstitution of hCD45⁺ cells. Three of five animals showed no symptoms of GVHD, two of five showed minor GVHD scores (Lockridge et al., 2013). Conversely, first-generation NeoThy mice that did not receive α hCD2 antibody died at multiple time points, beginning at 15 weeks post-humanization. As immunocompromised mice are prone to infections and other causes of death besides GVHD, large longitudinal cohorts of mice necropsied at time of death would be required to determine general susceptibility of the NeoThy to GVHD. As T cells begin to emerge at ~10–12 weeks post-humanization (Figure 2B), the experimental window for transplantation studies in the NeoThy may allow monitoring of transplanted grafts >20 weeks *in vivo*.

NeoThy mice created in NSG-W hosts using autologous thymus and HSCs, or with thymus and allogeneic HSCs, and in multiple donors with varying degrees of human leukocyte antigen (HLA) matching (Figure S2B) all robustly engrafted with human CD45⁺, CD19⁺, and CD3⁺ cells (Figure 2B). Both first- and second-generation protocols for NeoThy mice produce a typical component of hCD19⁺

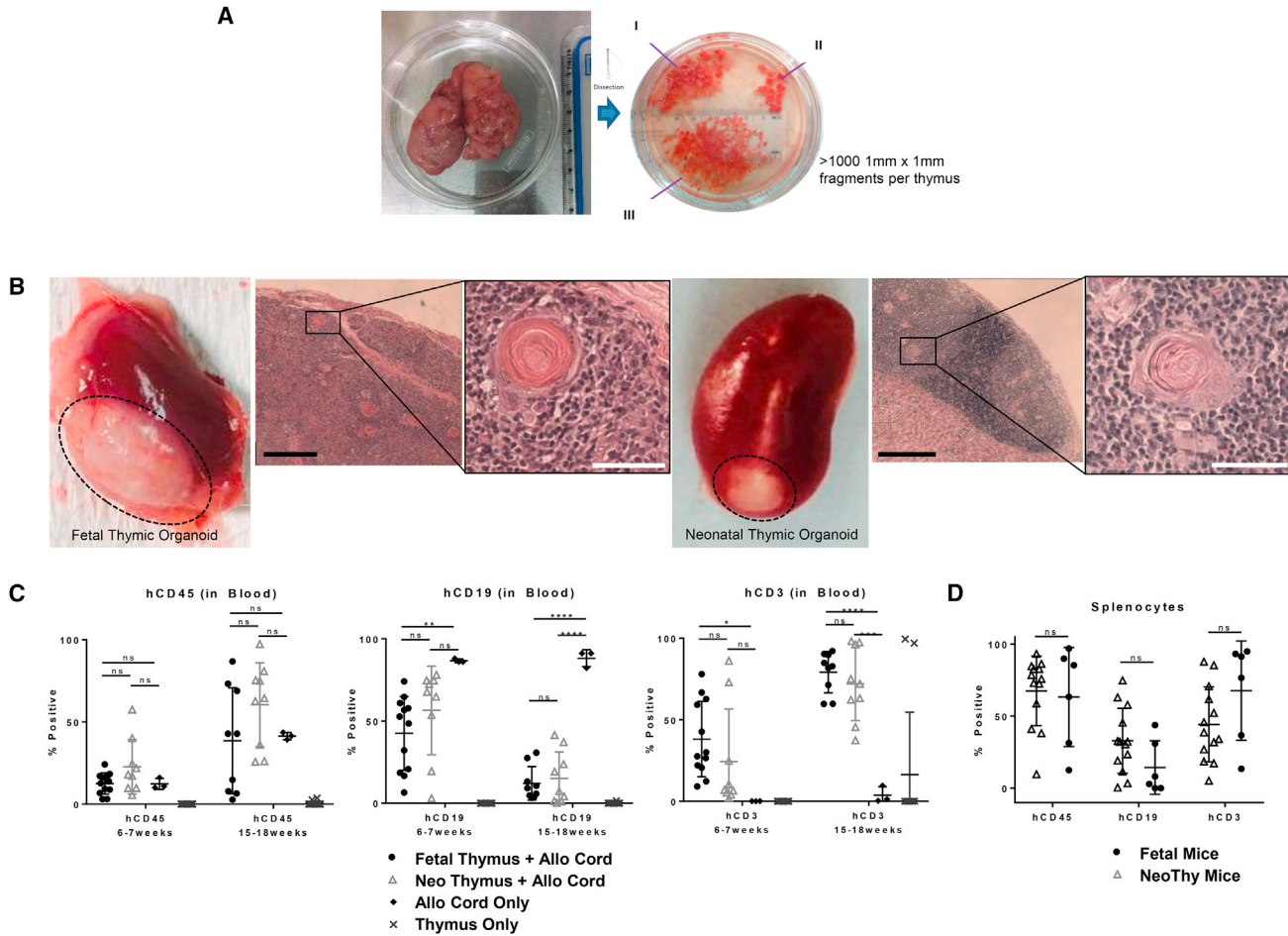


Figure 1. Engraftment of Human Thymus Tissue and Immune Cells

(A) Human neonatal thymus is abundant (e.g., 14.75 g, shown). Membrane, adipose, and blood vessels were removed and tissue processed into large (I), then medium (II), then 1 × 1 mm fragments (III) for cryopreservation. More than 1,000 fragments suitable for transplantation can be obtained from a single thymus.

(B) Implanted thymus fragments develop into organoids under the kidney capsule when co-transplanted i.v. with hCD34⁺ cells, +/- α hCD2 antibody depletion (second- and first-generation mice, respectively). Histological analysis of first-generation fetal humanized mouse (NSG) (left) and second-generation neonatal (NSG-W) (right) thymic organoids, including Hassall's corpuscles, are shown (4× scale bar, 500 μ m; inset is 10× scale bar, 100 μ m).

(C) Humanized mice were generated from various human tissue samples in irradiated NSG mice w/o α hCD2 antibody depletion (first generation) and compared for human immune cell engraftment (hCD45⁺), including B cells (hCD45⁺hCD19⁺) and T cells (hCD45⁺hCD3⁺) at early (6–7 weeks post-surgery) and late (15–18 weeks) time points. In four independent experiments, n = 12 animals received fetal thymus and allogeneic cord blood CD34⁺ cells (Fet Thymus + Allo Cord), n = 9 animals received neonatal thymus and allogeneic cord (Neo Thymus + Allo Cord), n = 3 allogeneic cord only (Allo Cord Only) and n = 12 neonatal thymus alone from 3 donors (Thymus Only). The Thymus Only condition did not receive hCD34⁺ cells. The Allo Cord Only condition received hCD34⁺ cells only.

(D) Splenocytes from fetal (n = 6) and neonatal tissue-derived (n = 13) first- and second-generation mice, using both NSG and NSG-W strains (seven independent experiments), were compared for human engraftment markers as in (C). Statistics were conducted using ANOVA, analyzed with GraphPad Prism 7.00. The Thymus Only control was included for comparison and was not analyzed for significance. ****p < 0.0001, ***p = 0.0001, **p < 0.01, *p < 0.05; ns, not significant; no bar, not analyzed. See also Figures S1, S2, and S3.

B cells and hCD3⁺ T cells, including hCD4⁺ and hCD8⁺ subsets (Figure 2C, additional data not shown). Additional human immune cell types relevant to transplant tolerance and rejection were consistently detected. Human

CD4⁺CD127^{lo}CD25⁺FOXP3⁺ regulatory T cells were observed in blood, spleen, and lung (Figure 2D), along with CD11b⁺, CD11c⁺, and CD14⁺ myeloid cells relevant for *in vivo* antigen presentation (Figure 2E). These data

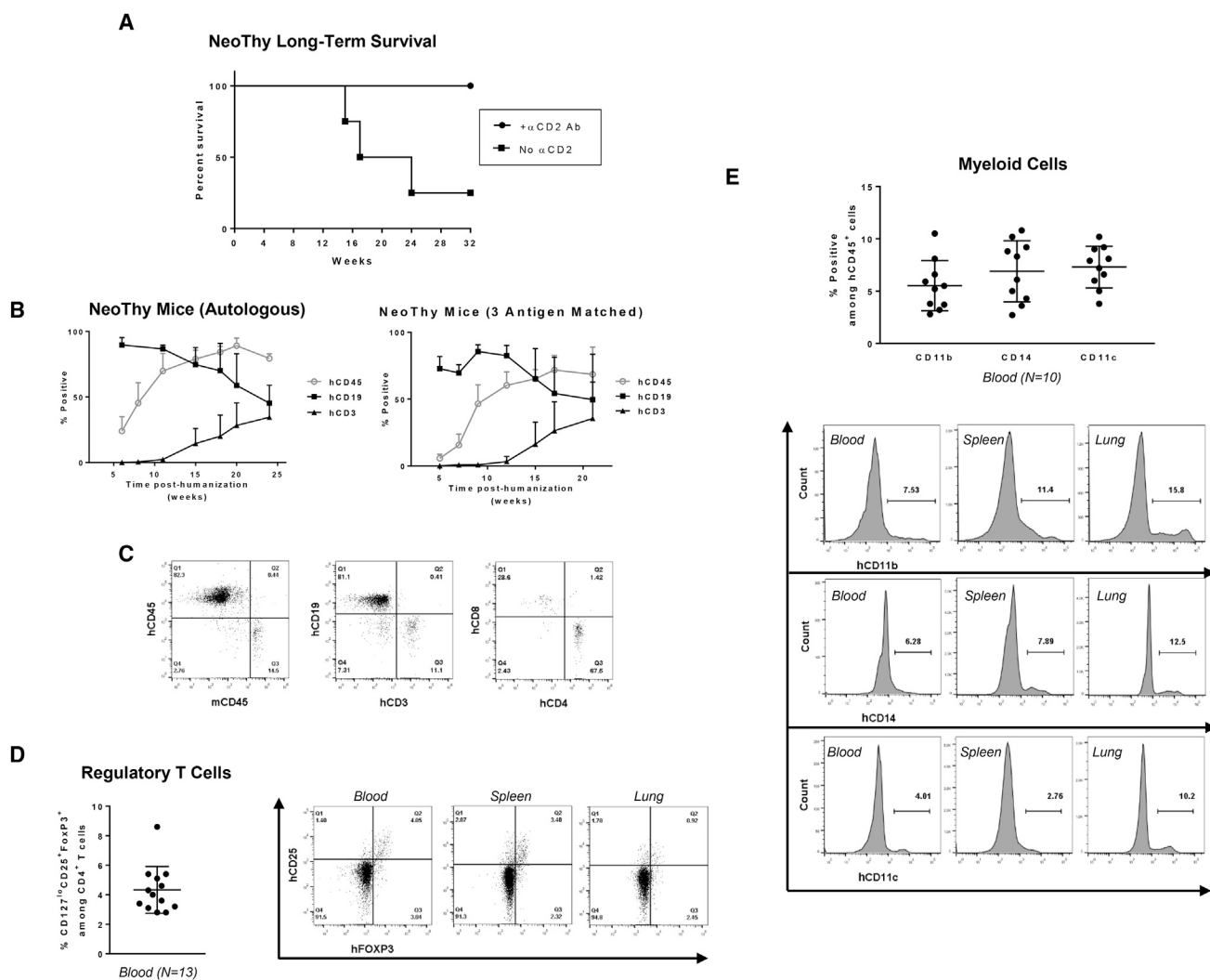


Figure 2. Long-Term Survival and Engraftment of Human Immune Cells in NeoThy Mice

(A) Five second-generation and four first-generation (+/- α hCD2 antibody, respectively) NeoThy (NSG-W) mice from the same experiment were humanized with neonatal thymus and allogeneic cord blood from one donor and followed for 32 weeks post-humanization, with no further experimental manipulations. Second-generation mice human immune cell reconstitution of hCD45⁺ cells was a mean of 61.6% \pm 17.0%, hCD45⁺hCD19⁺ cells, mean of 39.4% \pm 11.6%, and hCD45⁺hCD3⁺ cells, mean of 49.1% \pm 15.6% at experiment endpoint. First-generation mice reconstitution at 14 weeks (latest measurement prior to first animal death) for hCD45⁺ cells was a mean of 46.7% \pm 34.2%, hCD45⁺hCD19⁺ cells, mean of 24.2% \pm 21.2%, and hCD45⁺hCD3⁺ cells, mean of 41.1% \pm 26.8%. Statistics were conducted using Kaplan-Meier estimator method, compared with a log rank test, analyzed by GraphPad Prism 7.00 ($p = 0.0221$).

(B) Second-generation NeoThy (NSG-W) mice were humanized via implantation of neonatal thymus fragment and co-injection with either autologous (PED05, see Table S1) hCD34⁺ cells ($n = 10$ mice to start, 1 mouse removed at 17 weeks + 4 mice removed at 20 weeks $\rightarrow n = 5$ at endpoint, 2 pooled experiments) (left) or allogeneic hCD34⁺ cells matched at 1 allele each for HLA-A, -B, and -DR ($n = 12$ mice to start, 1 mouse removed at 15 weeks + 6 mice removed at 20 weeks $\rightarrow n = 5$ at endpoint, 1 experiment) (right) (PED05 + donor Allo Cord 212, see Table S1). Total human immune cell engraftment is shown over time. Error bars were determined using SD.

(C) Representative distributions of B and T cells are observed in blood of mice from (B) 18 weeks post-surgery.

(D) Human CD4⁺ hCD127^{lo}hCD25⁺hFOXP3⁺ surface and intracellular flow cytometry staining for regulatory T cells are shown compiled from one representative experiment of 13 second-generation NeoThy (NSG-W) mice engrafted with autologous PED05 tissues at 15 weeks and in representative second-generation NeoThy (NSG-W, allogeneic tissues) blood, spleen, and lungs at 17–29 weeks post-humanization.

(E) Peripheral blood from 1 experiment using 10 second-generation NeoThy (NSG-W, autologous PED05 tissue) mice at 15 weeks were compiled to show reproducibility within experiments (top panel) and representative staining from second-generation NeoThy (NSG-W, allogeneic tissues) is shown for blood, spleen, and lung cells stained for the myeloid cell markers hCD11b, hCD14, and hCD11c gated on viable single hCD45⁺ cells at 17–29 weeks (bottom panel). See also Figures S1, S2, and S3.



indicate that the NeoThy model harbors relevant cell populations for T cell responses; a primary mediator of transplant tolerance and allorejection.

Having shown robust engraftment of human T cells and other immune cells, we examined T cell function in the NeoThy model. *Ex vivo* engagement of T cell receptors with α hCD3, α hCD28, and rhIL2 stimulated T cell proliferation, indicated by blast-like clustering, dilution of CFSE dye in both CD4⁺ and CD8⁺ T cell populations, and production of Th1 cytokine interferon γ (Figures 3A and S2C). NeoThy mice reconstituted with human B and T cells also produced immunoglobulin G (IgG) and IgM antibodies (Figure 3B), indicating a functional T helper role of CD4⁺ T cells as well as functional B cells. Models of human T cell-mediated tolerance and rejection must demonstrate antigen-specific T cell function. Using the *trans vivo* delayed-type hypersensitivity assay, we show that NeoThy T cells mount a collagen V-specific effector response to co-injected antigen in the presence of anti-transforming growth factor β neutralizing antibody. This demonstrates the utility of the NeoThy for study of innate-like Th17 cell function in the context of iPSC immunogenicity (Sullivan et al., 2017). Last, NeoThy mice challenged with a B6 skin graft mounted rejection responses characterized by the two metrics of (1) hCD3⁺ T cell infiltration and (2) visible graft loss over time, similar to fetal tissue controls (Figures 3D and 3E). These data demonstrate the robust functional attributes of the T cell repertoire and the suitability of the NeoThy for pre-clinical investigations of iPSC immunogenicity.

To determine whether the NeoThy model could be used for *in vivo* investigation of allogeneic human iPSC immunogenicity, we reprogrammed NeoThy tissue donor cells into iPSCs. We successfully reprogrammed donor umbilical cord blood CD34-depleted cells (Figures S4A–S4F), and thymic stromal cells (data not shown) into iPSCs via a non-integrating episomal vector method (Yu et al., 2011). These iPSCs displayed conventional markers of pluripotency and were karyotypically normal. The cells were directly differentiated into cardiac troponin T-positive (cTNT) cardiomyocytes (CMs) (mean 75.5% cTNT⁺, ten differentiations of two donor lines) (Figure S4E). The iPSC-CMs spontaneously contracted in both 2D and 3D suspension cultures (Movies S1 and S2). iPSC-CMs from donor PED04 (Table S1) were transplanted under the kidney capsule of three second-generation NeoThy mice made with PED05 tissues and sacrificed 26 days later (Figure 4A).

NeoThy mice grafted with allogeneic iPSC-CMs showed macroscopic and histological retention of implanted cells (3/3) at the terminal time point and were infiltrated by human CD4⁺ and CD8⁺ T cells (Figure 4B). The lower degree of CD8⁺ infiltration observed could reflect

the higher ratio of peripheral blood CD4⁺ to CD8⁺ T cells seen in NeoThy (Figure 2C) and BLT (Rajesh et al., 2010) mice, and/or it could be due to the HLA-A2 match (associated with CD8⁺ T cell recognition) and HLA-DR mismatch (associated with CD4⁺ T cell recognition) between graft and recipient in the experiments.

Metrics for assessing rejection/tolerance of PSC therapies, in humanized mice and other models, vary among research groups and cell types (de Almeida et al., 2014; Kooreman et al., 2017; Sugita et al., 2016; Zhao et al., 2011). Progression of the field will require cell-type-specific criteria, informed by clinical solid organ transplantation guidelines (Haas, 2016; Solez et al., 1993). Our metric of graft infiltration can indicate a tolerance (de Almeida et al., 2014; Ling et al., 2015) or rejection response (Zhao et al., 2011). We cannot make a definitive conclusion about iPSC-CM transplant rejection, as this will require future studies at multiple time points corroborated with *in vitro* assays, such as the mixed lymphocyte reaction (Bach and Voynow, 1966) and other observations, such as graft destruction or disruption of function. Assessing mechanisms of graft infiltration in the NeoThy will be a key component of PSC immunogenicity studies going forward.

One previous report described humanizing animals with neonatal thymus, albeit without HSC co-injection (Barry et al., 1991). Our control data from Figure 1C (thymus-only) confirm their observations that thymic fragments are retained but without appreciable circulating human CD45⁺ cells. We did not observe human immune cells in our controls at early time points (6–7 weeks), and only 2 of 12 animals showed very low peripheral blood engraftment by 15–18 weeks (time point not measured by Barry et al., 1991). These later-emerging cells were overwhelmingly T cells, suggesting the emigration and homeostatic proliferation of passenger thymocytes from the thymic graft. In contrast, the robust circulating immune cells in the NeoThy are likely due to HSC co-injection coupled with human thymic education *in vivo*, as described below. The NSG-W host strain's more thorough immuno-depletion and/or use of quickly processed neonatal patient thymic explants may also have influenced our results.

A recently published report illustrated deficiencies in the T cell function of fetal BLT mice resulting in impaired alloimmune rejection of endothelial cells (Kooreman et al., 2017). This contrasts with our *ex vivo* assay of T cell proliferation following TCR stimulation (Figures 3A and S2C). We also tested the NeoThy versus fetal tissue control animals for markers associated with naive versus memory T cells (Figure S1C). We observed statistically significant differences in levels of CD45RA⁺ T cells among CD4⁺, but not CD8⁺, cells. In addition, there were smaller but statistically significant differences in the CD45RO⁺ T cells among

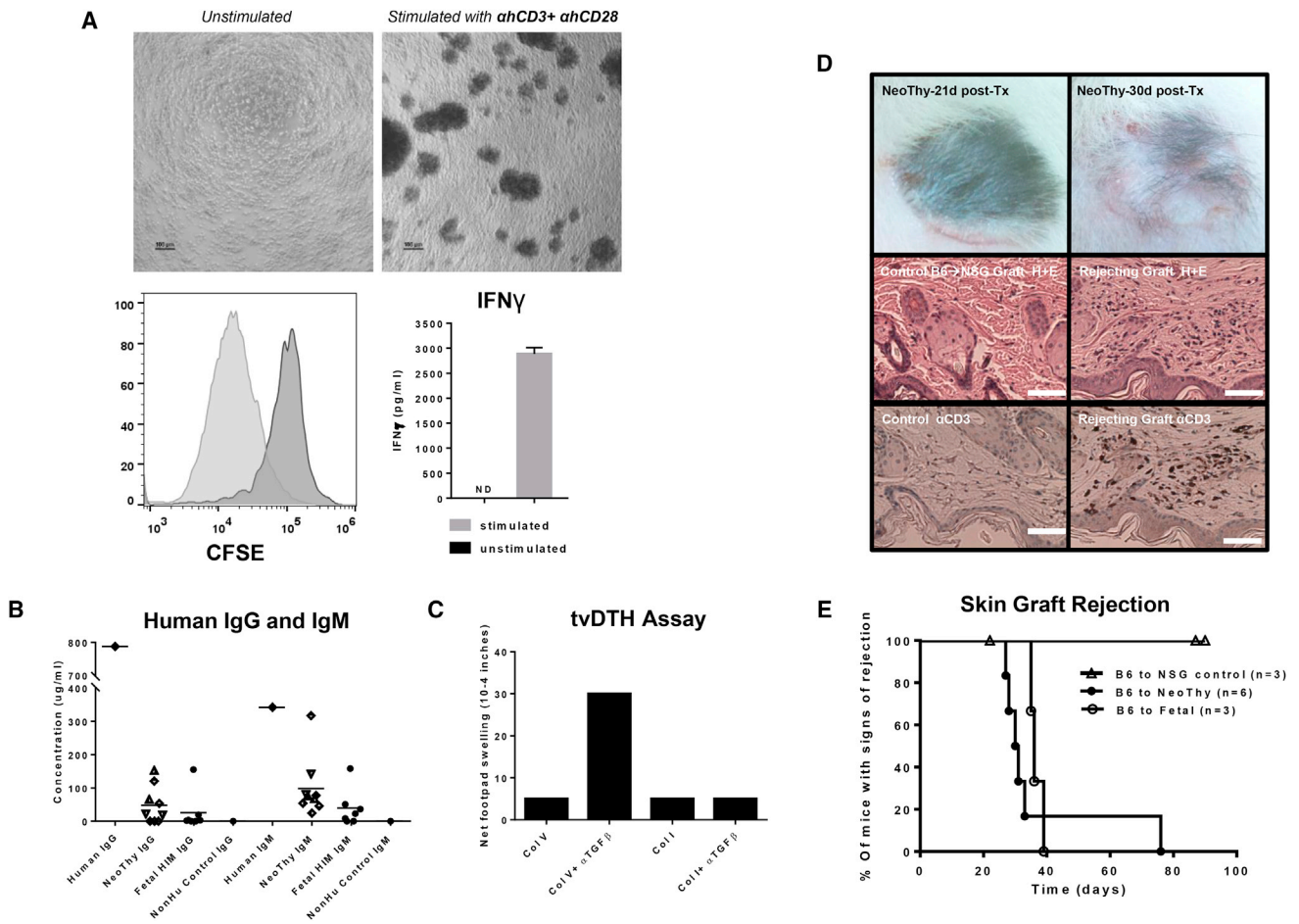


Figure 3. Human Immune Cell Function in the NeoThy

(A) *Ex vivo* splenic T cells from a representative second-generation NeoThy (NSG-W, allogeneic tissues) mouse were labeled with CFSE dye and stimulated with 5 μ g/mL α hCD3 (OKT3) antibody + α hCD28 + 300 IU/mL hIL2 and compared with unstimulated control with hIL2 alone. Flow cytometric analysis of CFSE dye dilution, gated on CD3⁺ cells, is shown: black line, unstimulated control; red line, stimulated condition, both at day 4 *ex vivo*. ELISA for human interferon γ (IFN- γ) was performed on day 4 cell culture supernatants. Error bars were determined using SD. ND, indicates no detection.

(B) Serum samples from 4 pooled independent experiments of second-generation NeoThy (NSG-W) (n = 9) and fetal thymus mice (n = 7) (both with allogeneic tissues) with verified B and T cell engraftment, 10–23 weeks post-humanization, were analyzed by ELISA for the concentration of human immunoglobulin G (IgG) and IgM antibodies. Healthy adult human serum (Hu Control) was used as a positive control. Statistics were conducted using ANOVA and no significant differences were found between fetal and NeoThy models for IgG or IgM.

(C) Antigen-specific T cell functionality in second-generation NeoThy (NSG-W) mice is measured by tvDTH assay via uncovering of a collagen V (Col V)-specific response after α transforming growth factor β (α TGF- β) Ab blocking.

(D and E) In one experiment, B6 mouse skin was grafted onto 12–14 weeks first-generation fetal (n = 3 mice) and NeoThy mice (n = 6, NSG, both allogeneic tissues), and non-humanized NSG controls (n = 3). Visible graft destruction (top right panel) and histological infiltration of hCD3⁺ T cells into rejecting B6 skin grafts (bottom right panel) is shown. Scale bars, 100 μ m (20 \times). Fetal tissue engrafted mice had a mean human immune cell reconstitution of 17.9% \pm 3.0% hCD45⁺ and 46.2% \pm 15.3% hCD45⁺hCD3⁺ and NeoThy mice had a mean of 68.6% \pm 27.3% hCD45⁺ and 49.2% \pm 27.6% hCD45⁺hCD3⁺ just prior to skin transplant surgery. Graft rejection was classified as presence of macroscopic lesions and hair loss for >5 days, coupled with hCD3⁺ infiltration. Statistics were conducted using Kaplan-Meier estimator method, compared with a log rank test, analyzed by GraphPad Prism 7.00. Differences were not significant. See also [Figures S1](#) and [S2](#).

CD8⁺, but not CD4⁺, cells. Future studies will explore whether these differences are biologically significant, e.g., if they impact the alloimmune response to various iPSC-derived cell types, and whether there are meaningful differ-

ences in lymphopenia-induced proliferation between the NeoThy and fetal models.

Interestingly, HLA-B58 disparity tracking experiments show that passenger thymocytes from thymus fragments

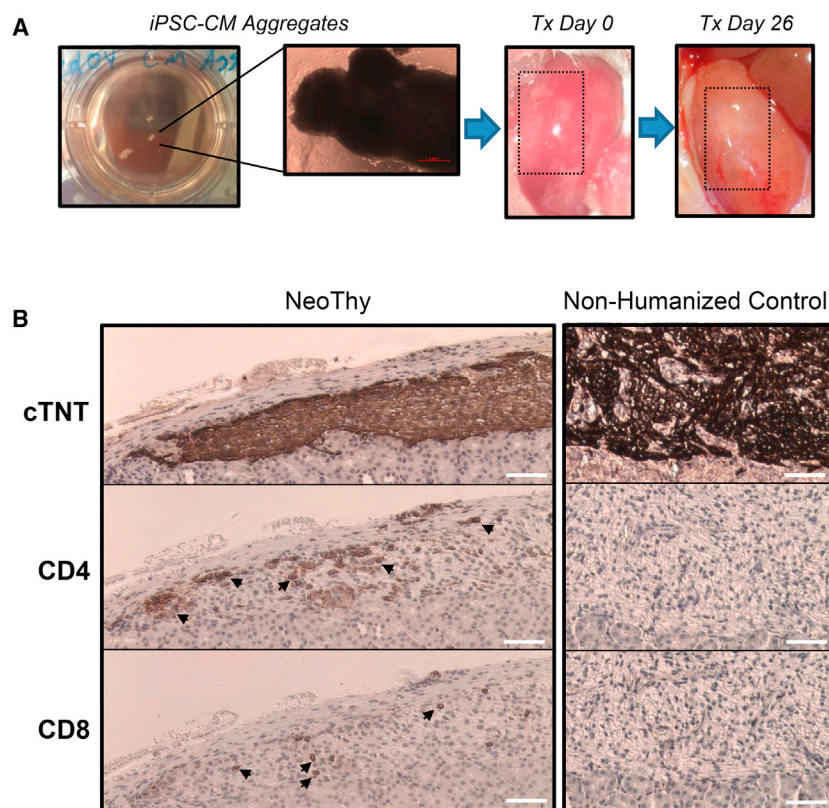


Figure 4. Transplantation of iPSC-Derived Cardiomyocytes in the NeoThy Mouse

(A) Contracting aggregates of allogeneic iPSC-cardiomyocytes (CMs) were transplanted under the right kidney capsule of second-generation NeoThy (NSG-W) mice (15 weeks post-humanization surgery), and non-humanized NSG-W controls. Engrafted CMs are visible (dotted boxes), on days 0 and 26 harvest.

(B) A representative image of immunohistochemical staining on day 26 grafts shows hCD4⁺ and hCD8⁺ T cells within the cTNT⁺ graft (black arrows). NeoThys had a mean of 84.4% ± 1.4% hCD45⁺ and 21.5% ± 26.0% hCD45⁺hCD3⁺ just prior to transplant surgery. All mice NeoThy and control mice retained transplanted graft 26 days *in vivo*. Scale bars, 100 μm (10×). See also Figure S4.

repopulate first-generation mice (not given α hCD2 antibody), in an early wave of hCD3⁺ T cell emergence (Figure S3). These mice have a mix of B58-positive and -negative T cells (Figure S3B, left plot), indicating both *de novo* T cell development from HSCs as well as passenger thymocyte emigration and proliferation. In contrast, second-generation mice (with α hCD2 antibody) (Figure S3B, right plot) exhibited a delay in T cell emergence and T cells uniformly expressed the HLA type of HSC source. This observation indicates the antibody-depleted passenger thymocytes from the thymic graft and these mice were reconstituted primarily with *de novo* T cells, as reported previously (Kalscheuer et al., 2012).

Using the clinically relevant metrics of immune cell frequency, and *ex vivo* and *in vivo* T cell function, the NeoThy humanized mouse model is a viable alternative to fetal tissue humanized mice. In addition to using the NeoThy for investigation of the immunogenicity of iPSC-derived cell therapies, the sheer abundance of neonatal thymic tissue allows for other intriguing applications. Recent breakthroughs in developing PSC-derived HSCs could be validated in the NeoThy (Sugimura et al., 2017). By investigating the T lymphopoietic potential of iPSC-derived HSCs educated by iPSC donors' thymic fragments, comparing them with autologous primary cord blood HSC controls (Wang et al., 1997).

The NeoThy model can play an integral role, in conjunction with *in vitro* assays of immunogenicity, in future studies investigating patient immune responses to self and allogeneic iPSC therapies and will also be of great value for hematopoiesis, transplant immunology, and virology research.

EXPERIMENTAL PROCEDURES

This work was approved by the Animal Care and Use Committee of the University of Wisconsin School of Medicine and Public Health and the Health Sciences Institutional Review Board, and complied with federal and state law. Humanized mice were generated similarly to previously published reports (Kalscheuer et al., 2012; Lan et al., 2006). In brief, 6- to 10-week-old immune-compromised 250 RAD irradiated NOD.*Prkdc*^{scid}*Il2Rγ*^{-/-} (NSG) and non-irradiated NOD.B6.SCID *Il2rγ*^{-/-}*Kit*^{W41/W41} (NBSGW, described in text as NSG-W) mice were used as host animals. Cryopreserved CD34-enriched HSCs were plated in SFEM medium (STEMCELL Technologies) plus 100 ng/mL rhStem Cell Factor (Miltenyi Biotech), and incubated at 37°C in 5% CO₂ overnight. The next day, 0.5–1.5 × 10⁵ HSCs were injected (i.v.) into anesthetized mice, coinciding with cryopreserved thymus fragment implantation surgery into the kidney capsule. A subset of mice also received i.v. α hCD2 antibody (100 μg) at days 0 and 7 post-surgery. Detailed methodology is available in the online Supplemental Experimental Procedures.



SUPPLEMENTAL INFORMATION

Supplemental Information includes Supplemental Experimental Procedures, four figures, one table, and two movies and can be found with this article online at <https://doi.org/10.1016/j.stemcr.2018.02.011>.

AUTHOR CONTRIBUTIONS

M.E.B. designed/performed experiments, analyzed data, and wrote the manuscript. Y.Z. designed/performed experiments and analyzed data. B.E.M. designed/performed experiments. I.G.N., H.E.L., M.B., and J.A.S. performed the experiments. P.V.A. performed cardiac surgery. T.J.K. and J.A.T. directed research, and W.J.B. directed research and edited the manuscript.

ACKNOWLEDGMENTS

Special thanks to the families who donated tissue for this research, to S. Babcock, and to P. Gianello for kindly providing the anti-CD2 hybridoma. This work was supported by the UW-Madison CMP program (NIH no. T32GM081061), UW ICTR (NIH no. UL1TR000427 and no. TL1TR000429), the UW Department of Surgery/Transplant Division (NIH no. 5T32AI125231-02), the NIH U01HL134764 (to T.J.K. and W.J.B.), UWSMPH, and the UW Stem Cell and Regenerative Medicine Center. See [Supplemental Experimental Procedures](#) for additional acknowledgments.

Received: August 23, 2017
Revised: February 20, 2018
Accepted: February 23, 2018
Published: March 22, 2018

REFERENCES

Bach, F.H., and Voynow, N.K. (1966). One-way stimulation in mixed leukocyte cultures. *Science* *153*, 545–547.

Barry, T.S., Jones, D.M., Richter, C.B., and Haynes, B.F. (1991). Successful engraftment of human postnatal thymus in severe combined immune deficient (SCID) mice: differential engraftment of thymic components with irradiation versus anti-asialo GM-1 immunosuppressive regimens. *J. Exp. Med.* *173*, 167–180.

Beaudin, A.E., Boyer, S.W., Perez-Cunningham, J., Hernandez, G.E., Derderian, S.C., Jujjavarapu, C., Aaserude, E., MacKenzie, T., and Forsberg, E.C. (2016). A transient developmental hematopoietic stem cell gives rise to innate-like B and T cells. *Cell Stem Cell* *19*, 768–783.

Bleul, C.C., Corbeaux, T., Reuter, A., Fisch, P., Monting, J.S., and Boehm, T. (2006). Formation of a functional thymus initiated by a postnatal epithelial progenitor cell. *Nature* *441*, 992–996.

Brehm, M.A., Cuthbert, A., Yang, C., Miller, D.M., Dilorio, P., Laning, J., Burzenski, L., Gott, B., Foreman, O., Kavirayani, A., et al. (2010). Parameters for establishing humanized mouse models to study human immunity: analysis of human hematopoietic stem cell engraftment in three immunodeficient strains of mice bearing the IL2 γ (null) mutation. *Clin. Immunol.* *135*, 84–98.

de Almeida, P.E., Meyer, E.H., Kooreman, N.G., Diecke, S., Dey, D., Sanchez-Freire, V., Hu, S., Ebert, A., Odegaard, J., Mordwinkin,

N.M., et al. (2014). Transplanted terminally differentiated induced pluripotent stem cells are accepted by immune mechanisms similar to self-tolerance. *Nat. Commun.* *5*, 3903.

Griesemer, A.D., Sorenson, E.C., and Hardy, M.A. (2010). The role of the thymus in tolerance. *Transplantation* *90*, 465–474.

Haas, M. (2016). The revised (2013) Banff classification for antibody-mediated rejection of renal allografts: update, difficulties, and future considerations. *Am. J. Transplant.* *16*, 1352–1357.

Hasini, H.S., Velichety, S.D., Thyagaraju, K., Jyothirmayi, K., and Jaipal Ch. (2014). Morphological features and morphometric parameters of human fetal thymus glands. *Int. J. Anat. Res.* *2*, 202–207.

Hu, Z., and Yang, Y.G. (2012). Full reconstitution of human platelets in humanized mice after macrophage depletion. *Blood* *120*, 1713–1716.

Kalscheuer, H., Danzl, N., Onoe, T., Faust, T., Winchester, R., Golland, R., Greenberg, E., Spitzer, T.R., Savage, D.G., Tahara, H., et al. (2012). A model for personalized in vivo analysis of human immune responsiveness. *Sci. Transl. Med.* *4*, 125ra130.

Kooreman, N.G., de Almeida, P.E., Stack, J.P., Nelakanti, R.V., Diecke, S., Shao, N.-Y., Swijnenburg, R.-J., Sanchez-Freire, V., Matsa, E., Liu, C., et al. (2017). Alloimmune responses of humanized mice to human pluripotent stem cell therapeutics. *Cell Rep.* *20*, 1978–1990.

Lan, P., Tonomura, N., Shimizu, A., Wang, S., and Yang, Y.G. (2006). Reconstitution of a functional human immune system in immunodeficient mice through combined human fetal thymus/liver and CD34+ cell transplantation. *Blood* *108*, 487–492.

Lavender, K.J., Pang, W.W., Messer, R.J., Duley, A.K., Race, B., Phillips, K., Scott, D., Peterson, K.E., Chan, C.K., Dittmer, U., et al. (2013). BLT-humanized C57BL/6 Rag2 $^{-/-}$ gammac $^{-/-}$ CD47 $^{-/-}$ mice are resistant to GVHD and develop B- and T-cell immunity to HIV infection. *Blood* *122*, 4013–4020.

Lee, H.M., Bautista, J.L., and Hsieh, C.S. (2011). Thymic and peripheral differentiation of regulatory T cells. *Adv. Immunol.* *112*, 25–71.

Ling, C., Li, Q., Brown, M.E., Kishimoto, Y., Toya, Y., Devine, E.E., Choi, K.O., Nishimoto, K., Norman, I.G., Tsegay, T., et al. (2015). Bioengineered vocal fold mucosa for voice restoration. *Sci. Transl. Med.* *7*, 314ra187.

Lockridge, J.L., Zhou, Y., Becker, Y.A., Ma, S., Kenney, S.C., Hematti, P., Capitini, C.M., Burlingham, W.J., Gendron-Fitzpatrick, A., and Gumperz, J.E. (2013). Mice engrafted with human fetal thymic tissue and hematopoietic stem cells develop pathology resembling chronic GVHD. *Biol. Blood Marrow Transplant.* *19*, 1310–1322.

McDermott, S.P., Eppert, K., Lechman, E.R., Doedens, M., and Dick, J.E. (2010). Comparison of human cord blood engraftment between immunocompromised mouse strains. *Blood* *116*, 193–200.

McGovern, N., Shin, A., Low, G., Low, D., Duan, K., Yao, L.J., Msallam, R., Low, I., Shadan, N.B., Sumatoh, H.R., et al. (2017). Human fetal dendritic cells promote prenatal T-cell immune suppression through arginase-2. *Nature* *546*, 662–666.



- McIntosh, B.E., and Brown, M.E. (2015). No irradiation required: the future of humanized immune system modeling in murine hosts. *Chimerism* 6, 40–45.
- McIntosh, B.E., Brown, M.E., Duffin, B.M., Maufort, J.P., Vereide, D.T., Slukvin, I.I., and Thomson, J.A. (2015). Nonirradiated NOD.B6.SCID IL2rgamma^{-/-} Kit(W41/W41) (NBSGW) mice support multilineage engraftment of human hematopoietic cells. *Stem Cell Reports* 4, 171–180.
- Mold, J.E., and McCune, J.M. (2012). Immunological tolerance during fetal development: from mouse to man. *Adv. Immunol.* 115, 73–111.
- Mold, J.E., Venkatasubrahmanyam, S., Burt, T.D., Michaelsson, J., Rivera, J.M., Galkina, S.A., Weinberg, K., Stoddart, C.A., and McCune, J.M. (2010). Fetal and adult hematopoietic stem cells give rise to distinct T cell lineages in humans. *Science* 330, 1695–1699.
- Notta, F., Zandi, S., Takayama, N., Dobson, S., Gan, O.I., Wilson, G., Kaufmann, K.B., McLeod, J., Laurenti, E., Dunant, C.F., et al. (2016). Distinct routes of lineage development reshape the human blood hierarchy across ontogeny. *Science* 351, aab2116.
- Rajesh, D., Zhou, Y., Jankowska-Gan, E., Roenneburg, D.A., Dart, M.L., Torrealba, J., and Burlingham, W.J. (2010). Th1 and Th17 immunocompetence in humanized NOD/SCID/IL2rgamma null mice. *Hum. Immunol.* 71, 551–559.
- Rong, Z., Wang, M., Hu, Z., Stradner, M., Zhu, S., Kong, H., Yi, H., Goldrath, A., Yang, Y.G., Xu, Y., et al. (2014). An effective approach to prevent immune rejection of human ESC-derived allografts. *Cell Stem Cell* 14, 121–130.
- Rongvaux, A., Willinger, T., Martinek, J., Strowig, T., Gearty, S.V., Teichmann, L.L., Saito, Y., Marches, F., Halene, S., Palucka, A.K., et al. (2014). Development and function of human innate immune cells in a humanized mouse model. *Nat. Biotechnol.* 32, 364–372.
- Saito, Y., Ellegast, J.M., Rafiei, A., Song, Y., Kull, D., Heikenwalder, M., Rongvaux, A., Halene, S., Flavell, R.A., and Manz, M.G. (2016). Peripheral blood CD34 cells efficiently engraft human cytokine knock-in mice. *Blood* 128, 1829–1833.
- Shultz, L.D., Brehm, M.A., Garcia-Martinez, J.V., and Greiner, D.L. (2012). Humanized mice for immune system investigation: progress, promise and challenges. *Nat. Rev. Immunol.* 12, 786–798.
- Shultz, L.D., Saito, Y., Najima, Y., Tanaka, S., Ochi, T., Tomizawa, M., Doi, T., Sone, A., Suzuki, N., Fujiwara, H., et al. (2010). Generation of functional human T-cell subsets with HLA-restricted immune responses in HLA class I expressing NOD/SCID/IL2r gamma(null) humanized mice. *Proc. Natl. Acad. Sci. USA* 107, 13022–13027.
- Solez, K., Axelsen, R.A., Benediktsson, H., Burdick, J.F., Cohen, A.H., Colvin, R.B., Croker, B.P., Droz, D., Dunnill, M.S., Halloran, P.F., et al. (1993). International standardization of criteria for the histologic diagnosis of renal allograft rejection: the Banff working classification of kidney transplant pathology. *Kidney Int.* 44, 411–422.
- Sugimura, R., Jha, D.K., Han, A., Soria-Valles, C., da Rocha, E.L., Lu, Y.F., Goettel, J.A., Serrao, E., Rowe, R.G., Malleshaiah, M., et al. (2017). Haematopoietic stem and progenitor cells from human pluripotent stem cells. *Nature* 545, 432–438.
- Sugita, S., Iwasaki, Y., Makabe, K., Kimura, T., Futagami, T., Suegami, S., and Takahashi, M. (2016). Lack of T cell response to iPSC-derived retinal pigment epithelial cells from HLA homozygous donors. *Stem Cell Reports* 7, 619–634.
- Sullivan, J.A., Jankowska-Gan, E., Hegde, S., Pestrak, M.A., Agashe, V.V., Park, A.C., Brown, M.E., Kernien, J.F., Wilkes, D.S., Kaufman, D.B., et al. (2017). Th17 responses to collagen type V, alpha1-tubulin, and vimentin are present early in human development and persist throughout life. *Am. J. Transplant.* 17, 944–956.
- Theocharides, A.P.A., Rongvaux, A., Fritsch, K., Flavell, R.A., and Manz, M.G. (2016). Humanized hemato-lymphoid system mice. *Haematologica* 101, 5–19.
- Wang, J.C.Y., Doedens, M., and Dick, J.E. (1997). Primitive human hematopoietic cells are enriched in cord blood compared with adult bone marrow or mobilized peripheral blood as measured by the quantitative in vivo SCID-repopulating cell assay. *Blood* 89, 3919–3924.
- Yu, J., Chau, K.F., Vodyanik, M.A., Jiang, J., and Jiang, Y. (2011). Efficient feeder-free episomal reprogramming with small molecules. *PLoS One* 6, e17557.
- Yu, J., Vodyanik, M.A., Smuga-Otto, K., Antosiewicz-Bourget, J., Frane, J.L., Tian, S., Nie, J., Jonsdottir, G.A., Ruotti, V., Stewart, R., et al. (2007). Induced pluripotent stem cell lines derived from human somatic cells. *Science* 318, 1917–1920.
- Zhao, T., Zhang, Z.N., Rong, Z., and Xu, Y. (2011). Immunogenicity of induced pluripotent stem cells. *Nature* 474, 212–215.
- Zhao, T., Zhang, Z.N., Westenskow, P.D., Todorova, D., Hu, Z., Lin, T., Rong, Z., Kim, J., He, J., Wang, M., et al. (2015). Humanized mice reveal differential immunogenicity of cells derived from autologous induced pluripotent stem cells. *Cell Stem Cell* 17, 353–359.